Circular Formation of Networked Dynamic Unicycles by a Distributed Dynamic Control Law ⋆

Xiao Yu, Xiang Xu, Lu Liu [1], Gang Feng

Department of Mechanical and Biomedical Engineering, City University of Hong Kong, Kowloon, Hong Kong SAR, China

Abstract

This paper investigates the circular formation control problem of networked dynamic unicycles. Each unicycle uses its local coordinate frame and the topology of the networked unicycles is modeled by a directed graph containing a spanning tree. A distributed dynamic control law is proposed for each unicycle based on the measurement via local sensing and the information of its neighbors via intermittent communication. It is shown that all unicycles can globally converge to the circular motion around a given center which is only known to one unicycle, and can globally converge to a desired spaced formation along the circle. Finally, simulation results of an example verify the effectiveness of the proposed control law.

Key words: Circular formation; Distributed control; Directed graph; Dynamic unicycles; Multi-agent systems.

1 Introduction

Recent decade witnesses the rapid development of distributed formation control (Oh et al., 2015), and graph theory has been extensively utilized in design and analysis (Hendrickx et al., 2007; Anderson et al., 2008). Significant effort has been devoted to formation control of multiple single-integrators, see Krick et al. (2009); Dorfler & Francis (2010); Oh & Ahn (2013); Lee & Ahn (2016) and references therein. However, these results cannot be applied to multiple unicycles due to the nonholonomic constraint. As the unicycle model can be used to describe the simplified model of a mobile wheeled robot (MWR) and an unmanned aerial vehicle (UAV) (Qu, 2009), interest in formation control of unicycles has been growing, and many works focus on circular formation control of multiple kinematic or dynamic unicycles.

For networked unicycles with all-to-all communication, Sepulchre et al. (2007) presented a comprehensive investigation on the circular formation of unicycles with unit linear velocity. Seyboth et al. (2014) studied the case where unicycles maintain nonidentical constant linear velocities. For the cyclic pursuit problem of multiple unicycles, it was shown in Marshall et al. (2004, 2006) that local stability of the closed-loop system can be established and the equilibrium corresponds to generalized regular polygons formation. Sinha & Ghose (2007) considered the case where unicycles are moving with different linear velocities. Zheng et al. (2009) proposed a projection-based control law and ensured that the trajectories of unicycles will not diverge. For unicycles in the cyclic pursuit manner, many works focused on the case where the center of the common circle is given and known to all unicycles. Ceccarelli et al. (2008) took into account the limited visibility region of onboard sensors, and Summers et al. (2009) addressed the spaced formation along the circle based on the rigidity of graphs. Lan et al. (2010) developed a hybrid control law for a target-enclosing task. Zheng et al. (2015) proposed controllers based on bearing-only measurement. For the case where the center is only known to one unicycle, Yu & Liu (2016a) proposed a distributed dynamic control law for ring-networked unicycles. Several works investigated the circular formation of unicycles under a network of more general topology. Sepulchre et al. (2008) proposed a dynamic control law based on a balanced graph condition. Chen & Zhang (2011, 2013) developed a controller based on a jointly connected condition for unicycles under a proximity graph. Note that all aforementioned approaches were developed for kinematic unicycles. While for dynamic unicycles, El-Hawwary & Maggiore (2013) proposed a hierarchical

⋆ This work was supported by the Research Grants Council of the Hong Kong Special Administrative Region of China under Project CityU/11213415. The material in this paper was not presented at any conference.

Email addresses: xiaoyu4-c@my.cityu.edu.hk (Xiao Yu), xiangxu5-c@my.cityu.edu.hk (Xiang Xu), luliu45@cityu.edu.hk (Lu Liu), megfeng@cityu.edu.hk (Gang Feng).

[1] Tel.: +852-3442-5426; Fax: +852-3442-0172.

Author version of DOI:10.1016/j.automatica.2017.11.021

controller design strategy, such that unicycles achieve a circular formation with a desired spacing.

In this paper, we consider a formation control problem of networked dynamic unicycles with respect to a given center only known to one unicycle. The major challenge is to develop a distributed control law for unicycles of which the network topology is a directed graph, such that the global asymptotic stability of the closed-loop system corresponding to a circular formation with any desired spacing can be established. To overcome it, a dynamic control law with a feasible estimate of the center is proposed, and it requires each unicycle to use both sensing and communication, as in Oh & Ahn (2013).

The contribution of this paper mainly lies in the following four aspects. First, the aforementioned results on circular formation of kinematic unicycles cannot be directly extended to dynamic unicycles. In fact, our proposed control law makes dynamic unicycles reduced to kinematic unicycles, which implies that the control law design can be applied to kinematic unicycles. Second, a directed graph with a spanning tree is a more general assumption than most existing works, for example, a complete graph (Sepulchre et al., 2007; Seyboth et al., 2014), a balanced graph (Sepulchre et al., 2008), a cycle (Marshall et al., 2004, 2006; Zheng et al., 2009; Summers et al., 2009; Yu & Liu, 2016a), and a connected undirected graph (El-Hawwary & Maggiore, 2013). Third, the assumption that only one unicycle knows the center is obviously less restrictive than the one that all unicycles know the center (Sepulchre et al., 2007; Ceccarelli et al., 2008; Summers et al., 2009; Lan et al., 2010; Zheng et al., 2015). Some works considered an unspecified center (Marshall et al., 2004, 2006; Sepulchre et al., 2007, 2008; Zheng et al., 2009; Chen & Zhang, 2011, 2013; Seyboth et al., 2014; El-Hawwary & Maggiore, 2013), and those results can be extended to the case where only one unicycle knows a given center, by letting a unicycle orbit around the center as the so-called "stubborn" one in Chen & Zhang (2011). However, the stability of the closed-loop system was established on a linearized system (Marshall et al., 2004, 2006; Zheng et al., 2009) or an approximated system (Chen & Zhang, 2011, 2013). While our proposed control law guarantees the global asymptotic stability of the original closed-loop system. Finally, noting that in the aforementioned works, only El-Hawwary & Maggiore (2013) considered the circular formation with any desired spacing, and made unicycles locally converge to a desired spaced formation when the sensor graph is directed. While with our proposed control law, unicycles can achieve global convergence to any desired spaced formation along the circle.

The rest of this paper is organized as follows. In Section 2, the problem formulation and three technical lemmas are given. Section 3 presents the main results and Section 4 shows the simulation results of an illustrative example. Finally, the conclusion is drawn in Section 5.

Notations: Throughout the paper, $\|\boldsymbol{x}\|$ denotes the 2–norm of a vector $\boldsymbol{x} \in \mathbb{R}^n$.

2 Preliminaries

2.1 Problem Formulation

Consider N dynamic unicycles in the form of:

$$\begin{aligned} &\dot{x}_i = v_i \cos\theta_i,\ \dot{y}_i = v_i \sin\theta_i,\ \dot{\theta}_i = \omega_i, \\ &\dot{v}_i = F_i/I,\ \dot{\omega}_i = T_i/J,\ i = 1, ..., N, \end{aligned} \tag{1}$$

where $\boldsymbol{p}_i := [x_i\ y_i]^{\mathrm{T}} \in \mathbb{R}^2$ is the coordinate of the position and $\theta_i \in \mathbb{R}$ is the heading angle of unicycle i in the inertial frame, $v_i \in \mathbb{R}$ and $\omega_i \in \mathbb{R}$ are the linear velocity and the angular velocity respectively. The control inputs are the torques F_i and T_i, and I and J are constants associated with the moments of inertia.

All unicycles are anonymous and each one only has access to the information of its neighbors in a network. The network topology is described by a directed graph $\mathcal{G} = \{\mathcal{O}, \mathcal{E}\}$ as follows. Digraph $\mathcal{G}$ consists of a finite set of nodes $\mathcal{O} = \{1, ..., N\}$ representing N unicycles, and a set of edges $\mathcal{E} \subseteq \{(j,i) : j \neq i, i, j \in \mathcal{O}\}$ containing directed edges from node j to node i. A directed edge (j,i) means that the information of unicycle j is available to unicycle i. Denote the Laplacian matrix of $\mathcal{G}$ by matrix $\mathcal{L}$. The following assumption is made on $\mathcal{G}$:

Assumption 1 Digraph $\mathcal{G}$ contains a directed spanning tree with one node, namely node l, being the root. ■

The network is physically set up by the sensors and communication devices of each unicycle. The network topology at an instant t can be further described by a sensor graph $\mathcal{G}_s(t) = \{\mathcal{O}, \mathcal{E}_s(t)\}$ and a communication graph $\mathcal{G}_c(t) = \{\mathcal{O}, \mathcal{E}_c(t)\}$. Define the sets $\mathcal{N}_c^i(t)$ and $\mathcal{N}_s^i(t)$ as $\mathcal{N}_c^i(t) = \{j \in \mathcal{O} | (j,i) \in \mathcal{E}_c(t)\}$ and $\mathcal{N}_s^i(t) = \{j \in \mathcal{O} | (j,i) \in \mathcal{E}_s(t)\}$ respectively. Finally, denote the Laplacian matrices of $\mathcal{G}_s(t)$ and $\mathcal{G}_c(t)$ by $\mathcal{L}_s(t)$ and $\mathcal{L}_c(t)$ respectively. Assume that $\mathcal{G}_s(t)$ is time-invariant as in El-Hawwary & Maggiore (2013) and $\mathcal{G}_c$ is allowed to be time-varying. Then, the following assumption is made.

Assumption 2 There exists an infinite sequence of nonempty, continuous, uniformly bounded and non-overlapping time intervals $[t_n, t_{n+1}),\ n = 0, 1, ...,$ with $t_{n+1} - t_n \leq \bar{T}$ for some $\bar{T} > 0$. In each $[t_n, t_{n+1})$, there exists a finite sequence of nonempty and continuous time subintervals $[t_n^k, t_n^{k+1}),\ k = 0, 1, ..., k_n - 1$, with $t_n^0 = t_n$, $t_n^{k_n} = t_{n+1}$ and $t_n^{k+1} - t_n^k \geq \bar{\tau}$ for $\bar{\tau} > 0$ and an integer k_n. $\mathcal{G}_c(t)$ does not change during each $[t_n^k, t_n^{k+1})$, and the union graph of $\mathcal{G}_c(t)$ during each $[t_n, t_{n+1})$ is $\mathcal{G}$, i.e., $\bigcup_{j=0}^{j=k_n-1} \mathcal{G}_c(t_n^j) = \mathcal{G},\ n = 0, 1, ...$ While the sensor graph $\mathcal{G}_s(t)$ satisfies $\mathcal{G}_s(t) = \mathcal{G}$ for all $t \geq t_0$. ■

For the local sensing, when the inertial frame or a common reference direction (Lin et al., 2004) is unavailable, the sensors cannot obtain $\boldsymbol{p}_i$, $\boldsymbol{p}_j$, or $\boldsymbol{p}_i - \boldsymbol{p}_j$, $j \in \mathcal{N}_i$. In this case, each unicycle can establish its local coordinate frame as in El-Hawwary & Maggiore (2013), i.e., the Frenet-Serret frame. Then, $\boldsymbol{p}_j$, $\boldsymbol{q}_0$, and θ_j, $j \in \mathcal{N}_i$, measured by unicycle i can be expressed as

$$\boldsymbol{p}_j^i = R(\theta_i)(\boldsymbol{p}_j - \boldsymbol{p}_i), \boldsymbol{q}_0^i = R(\theta_i)(\boldsymbol{q}_0 - \boldsymbol{p}_i), \theta_j^i = \theta_j - \theta_i,$$

respectively, where $R(\cdot) = \begin{bmatrix} \cos(\cdot) & \sin(\cdot) \\ -\sin(\cdot) & \cos(\cdot) \end{bmatrix}$.

Circular formation control aims at making all unicycles achieve the following objectives: (i) orbiting along a common circle with the center $\boldsymbol{q}_0 := [x_0 \ y_0]^{\mathrm{T}}$ and radius r; (ii) maintaining a desired spaced formation described by a vector $\boldsymbol{\alpha} \in \mathbb{R}^N$ along the common circle; (iii) moving with a constant angular velocity ϖ. The vector $\boldsymbol{\alpha} = [\alpha_1, ..., \alpha_N]^{\mathrm{T}}$ is used to describe the desired separation angle of two unicycles with respect to the center. $\boldsymbol{\alpha}$ can be set as $\alpha_1 = 0$, $\alpha_N \leq 2\pi$, and $\alpha_i \leq \alpha_{i+1}$, $i = 1, ..., N-1$. Then, $\alpha_{ji} := \alpha_j - \alpha_i$ can be viewed as the desired separation angle between unicycles i and j with respect to the center. The *circular formation control problem* in this paper is formally defined as follows.

Problem 1 Consider N networked dynamic unicycles (1). Given a digraph $\mathcal{G}$, a circular formation center $\boldsymbol{q}_0 \in \mathbb{R}^2$, a radius r, and a constant vector $\boldsymbol{\alpha} \in \mathbb{R}^N$ describing the desired spacing, for unicycle i, $i = 1, ..., N$, with any initial states $[\boldsymbol{p}_i^{\mathrm{T}}(t_0) \ \theta_i(t_0) \ v_i(t_0) \ \omega_i(t_0)]^{\mathrm{T}} \in \mathbb{R}^5$, $\forall t_0 \geq 0$, find a distributed dynamic control law in the form of

$$[F_i \ T_i]^{\mathrm{T}} = \boldsymbol{\sigma}(\boldsymbol{\rho}_i^i, \boldsymbol{p}_j^i, \theta_j^i, \omega_{ji}, r, \alpha_{ji}), \quad (2)$$

$$\dot{\boldsymbol{\rho}}_i^i = \boldsymbol{\kappa}(\boldsymbol{\rho}_i^i, \boldsymbol{\rho}_j^j, \boldsymbol{p}_j^i, \theta_j^i, r, \alpha_{ji}), \ j \in \mathcal{N}_i, \quad (3)$$

such that

$$\lim_{t\to\infty} (\boldsymbol{p}_i(t) - \boldsymbol{q}_0) = r[\sin\theta_i(t) \ -\cos\theta_i(t)]^{\mathrm{T}}, \quad (4)$$

$$\lim_{t\to\infty} (\mathcal{L}_s(t)(\boldsymbol{\theta}(t) - \boldsymbol{\alpha})) \in \mathcal{S}, \ \boldsymbol{\theta} = [\theta_1, ..., \theta_N]^{\mathrm{T}}, \quad (5)$$

$$\lim_{t\to\infty} \omega_i(t) = \varpi, \ \lim_{t\to\infty} v_i(t) = \varpi r, \quad (6)$$

where r and ϖ are given positive constants, $\boldsymbol{\rho}_i^i$, to be designed later, is an internal state measured in the local coordinate frame, $\omega_{ji} := \omega_j - \omega_i$ is the relative angular velocity of the neighbors, α_{ji} denotes the desired relative spacing to the neighbors and is defined as $\alpha_{ji} := \alpha_j - \alpha_i$ with α_i being the ith entry of $\boldsymbol{\alpha}$, set $\mathcal{S}$ is defined as $\mathcal{S} = \{\boldsymbol{\theta} \in \mathbb{R}^N : \mathcal{L}_s(\boldsymbol{\theta} - \boldsymbol{\alpha}) = \mathbf{0} \bmod 2\pi\}$. Moreover, functions $\boldsymbol{\sigma}(\cdot)$ and $\boldsymbol{\kappa}(\cdot)$ are both sufficiently smooth. ■

In Problem 1, (4), (5), and (6) describes the aforementioned objectives (i), (ii), and (iii) respectively. Note that the separation angle for each pair of unicycles equals the relative heading angle (modulo 2π) when the pair of unicycles moves along a common circle. Besides, Problem 1 is investigated under the following assumptions.

Assumption 3 Only one unicycle l knows the center in its local coordinate frame at the initial time t_0, i.e., only $\boldsymbol{q}_0^l(t_0)$ is known to unicycle l. In digraph $\mathcal{G}$, node l has zero in-degree. ■

Assumption 4 Each unicycle knows its own initial velocities, i.e., $v_i(t_0)$ and $\omega_i(t_0)$. ■

Remark 1 Assumption 1 and $\mathcal{G}_s(t) = \mathcal{G}$, $\forall t \geq t_0$, in Assumption 2 are also used in El-Hawwary & Maggiore (2013). Assumption 2 implies that the communication among unicycles are allowed to be intermittent. Under Assumption 3, the center of the circle $\boldsymbol{q}_0$ can be prespecified and is only known to one unicycle. While in El-Hawwary & Maggiore (2013), $\boldsymbol{q}_0$ is not prespecified and is dependent on the initial positions of unicycles. ■

Remark 2 The required measurements in this paper are more restrictive than that in some existing results on circular formation of kinematic unicycles. For example, Marshall et al. (2004, 2006); Zheng et al. (2009); Lan et al. (2010); Zheng et al. (2015) did not need relative heading angle measurements. However, these results cannot be directly extended to dynamic unicycles. For circular formation of dynamic unicycles, El-Hawwary & Maggiore (2013) also used relative heading angle and relative angular velocity measurements, i.e., θ_j^i and ω_{ji}. Compared with El-Hawwary & Maggiore (2013), our proposed control law only requires each unicycle to measure its velocities at initial time instead of for all time, which further reduces the requirement on measurements. The relative heading angle and relative angular velocity measurements can be obtained by using an Attitude and Heading Reference System (AHRS), for example, the one implemented in Wang et al. (2014). ■

2.2 Technical Lemmas

We now introduce three technical lemmas which are used in the next section.

The first lemma is on the stability of continuous-time adaptive systems Narendra & Annaswamy (1987).

Lemma 1 A system $\dot{\boldsymbol{x}} = \begin{bmatrix} A & -b\boldsymbol{u}^{\mathrm{T}}(t) \\ u(t)b^{\mathrm{T}} & 0 \end{bmatrix}$, where $\boldsymbol{x} = [\boldsymbol{x}_1^{\mathrm{T}} \ \boldsymbol{x}_2^{\mathrm{T}}]^{\mathrm{T}}$, $\boldsymbol{x}_1 \in \mathbb{R}^m$, $\boldsymbol{x}_2 \in \mathbb{R}^n$, $A \in \mathbb{R}^{m\times m}$ is an stable matrix with $A + A^{\mathrm{T}}$ being negative definite, (A, b) is controllable, and $\boldsymbol{u} : \mathbb{R}_{\geq 0} \to \mathbb{R}^n$ is piecewise-continuous and bounded. The equilibrium of this system is globally exponentially stable if and only if $\boldsymbol{u}(t)$ is persistently exciting, i.e., there exist positive constants t_0, T_0, and α such that $\int_t^{t+T_0} \boldsymbol{u}(\tau)\boldsymbol{u}^{\mathrm{T}}(\tau)d\tau \geq \alpha \boldsymbol{I}$, $\forall t \geq t_0$. ■

The second lemma can be obtained by Theorem 1 in Zhang et al. (2015).

Lemma 2 Suppose that Assumption 1 holds and let node 1 denote the root in digraph $\mathcal{G}$. Assume that node 1 has no incoming edges from other nodes. Define $\underline{A} = \mathrm{diag}(a_{21}, ..., a_{N1})$, where $a_{i1} = 1$, $i \geq 2$, if there is an edge $(1, i)$; $a_{i1} = 0$, otherwise. Denote $\underline{\mathcal{L}}$ as the Laplacian matrix of digraph $\underline{\mathcal{G}} = (\mathcal{O}\backslash\{1\}, \mathcal{E}\backslash\{(1, j)|j \in \mathcal{O}, j \neq 1\})$. Let $\boldsymbol{\eta} = [\eta_2, ..., \eta_N]^{\mathrm{T}} = (\underline{\mathcal{L}} + \underline{A})^{-1}\mathbf{1}$, $\boldsymbol{\zeta} = [\zeta_2, ..., \zeta_N]^{\mathrm{T}} = (\underline{\mathcal{L}} + \underline{A})^{-\mathrm{T}}\mathbf{1}$, $P = \mathrm{diag}(p_2, ..., p_N)$ with $p_i = \zeta_i/\eta_i$, and

$Q = P(\underline{\mathcal{L}} + \underline{\mathcal{A}}) + (\underline{\mathcal{L}} + \underline{\mathcal{A}})^{\mathrm{T}} P$. Then, P and Q are both positive definite. ■

The third lemma can be referred to as a comparison principle for vectorial differential equations. Say that $\boldsymbol{x} \leq \boldsymbol{y}$ for $\boldsymbol{x},\ \boldsymbol{y} \in \mathbb{R}^n$ if the entries of $\boldsymbol{x}$ and $\boldsymbol{y}$ satisfy $x_i \leq y_i$, $i = 1, ..., n$.

Lemma 3 Consider the vectorial differential equation $\dot{\boldsymbol{y}} = \boldsymbol{f}(t, \boldsymbol{y})$ with $\boldsymbol{y} = [y_1, ..., y_n]^{\mathrm{T}} \in \mathbb{R}^n$ and $\boldsymbol{f}(t, \boldsymbol{y}) = [f_1(t, \boldsymbol{y}), ..., f_n(t, \boldsymbol{y})]^{\mathrm{T}}$, where $f_i(t, \boldsymbol{y})$ is differentiable in t and locally Lipschitz in $\boldsymbol{y}$, for all $t \geq t_0$ and all $\boldsymbol{y} \in \Psi$ with Ψ being any subset of $\mathbb{R}^n$. Let $[t_0, T)$ (T could be infinity) be the maximal interval of existence of the solution $\boldsymbol{y}(t)$ and suppose $\boldsymbol{y}(t) \in \Psi$ for all $t \in [t_0, T)$. Let $\boldsymbol{x}(t) \in \mathbb{R}^n$ be a continuous function of which the upper right-hand derivative $\mathrm{D}^+\boldsymbol{x}(t)$ satisfies

$$\mathrm{D}^+\boldsymbol{x}(t) \leq \boldsymbol{f}(t, \boldsymbol{x}(t)), \quad \boldsymbol{x}(t_0) \leq \boldsymbol{y}(t_0), \tag{7}$$

with $\boldsymbol{x}(t) \in \Psi$ for all $t \in [t_0, T)$. Then, $\boldsymbol{x}(t) \leq \boldsymbol{y}(t)$ for all $t \in [t_0, T)$ if for any $i \neq j$, $\frac{\partial f_i(t, \boldsymbol{x})}{\partial x_j} \geq 0$. ■

The proof is given in Appendix.

3 Main Results

In this section, the solution to the *circular formation control problem* is given.

Define the tracking error $\boldsymbol{p}_{ei} := [x_{ei}\ y_{ei}]^{\mathrm{T}}$ as $\boldsymbol{p}_{ei} = R(\theta_i)(\boldsymbol{q}_0 - \boldsymbol{p}_i + r[\sin\theta_i\ \ -\cos\theta_i]^{\mathrm{T}})$, i.e.,

$$\boldsymbol{p}_{ei} = \boldsymbol{q}_0^i + rP, \tag{8}$$

where P is a constant vector as $P = [0\ \ -1]^{\mathrm{T}}$.

Thus, to solve Problem 1, it suffices to design $[F_i\ T_i]^{\mathrm{T}}$ such that (i) $\boldsymbol{p}_e = [\boldsymbol{p}_{e1}^{\mathrm{T}}, ..., \boldsymbol{p}_{eN}^{\mathrm{T}}]^{\mathrm{T}}$ converges to zero for any initial $\boldsymbol{p}_{ei}(t_0) \in \mathbb{R}^2,\ i = 1, ..., N$; (ii) $\boldsymbol{\theta}$ converges to set $\mathcal{S}$ for any initial $\boldsymbol{\theta}(t_0) \in \mathbb{R}^N$.

However, under Assumption 2, unicycle i, $i \neq l$, does not have any knowledge of $\boldsymbol{q}_0^i$ or $\boldsymbol{p}_{ei}$. In this case, an estimate of the center in the coordinate frame of unicycle i is set, and is expressed as $\hat{\boldsymbol{q}}_0^i \in \mathbb{R}^2$.

The basic idea of control law design is first to make the dynamic unicycle (1) purely kinematic with the velocities being new inputs, then to design the velocities such that each unicycle can converge to the desired circular motion around its estimate of the center, and finally to develop a dynamic update law for the estimate such that all estimates can converge to the actual values.

Then, a dynamic control law is proposed as follows.

$$F_i = I\dot{\hat{\omega}}_i r + Ik_1k_2b_i r\,\mathrm{sech}^2(k_2b_i\sum_{j\in\mathcal{N}_s^i(t)}(\theta_j^i - \alpha_{ji}))\sum_{j\in\mathcal{N}_s^i(t)}\omega_{ji}, \tag{9}$$

$$T_i = \frac{JF_i}{Ir} - \frac{J\mu_i\nu_i}{r}Q^{\mathrm{T}}\dot{\hat{\boldsymbol{q}}}_0^i\,\mathrm{sech}^2(\nu_i Q^{\mathrm{T}}\hat{\boldsymbol{q}}_0^i), \tag{10}$$

$$\begin{aligned}\dot{\hat{\boldsymbol{q}}}_0^i &= k_3\sum_{j\in\mathcal{N}_c^i(t)}a_{ij}(t)(R(-\theta_j^i)\hat{\boldsymbol{q}}_0^j + \boldsymbol{p}_j^i - \hat{\boldsymbol{q}}_0^i) \\ &\quad + \bar{\omega}_i S\hat{\boldsymbol{q}}_0^i - \bar{v}_i Q, \quad i \neq l, \qquad (11)\\ \dot{\hat{\boldsymbol{q}}}_0^l &= \bar{\omega}_l S\hat{\boldsymbol{q}}_0^l - \bar{v}_l Q + k_3(\hat{\boldsymbol{q}}_0^l - \check{\boldsymbol{q}}_0^l), \qquad (12)\\ \dot{\check{\boldsymbol{q}}}_0^l &= \bar{\omega}_l S\check{\boldsymbol{q}}_0^l - \bar{v}_l Q, \qquad (13)\\ \dot{\hat{\omega}}_i &= k_4(\varpi - \hat{\omega}_i), \qquad (14)\end{aligned}$$

with $\bar{v}_i$ and $\bar{\omega}_i$ being defined as

$$\bar{v}_i = \hat{\omega}_i r + k_1 r\tanh(k_2b_i\sum_{j\in\mathcal{N}_s^i(t)}(\theta_j^i - \alpha_{ji})), \tag{15}$$

$$\bar{\omega}_i = \bar{v}_i/r - \mu_i\tanh(\nu_i Q^{\mathrm{T}}\hat{\boldsymbol{q}}_0^i)/r, \tag{16}$$

where $\hat{\omega}_i \in \mathbb{R}$ and $\check{\boldsymbol{q}}_0^l \in \mathbb{R}^2$ are internal states, k_1–k_4, μ_i and ν_i are positive constants, $S = \begin{bmatrix} 0 & 1 \\ -1 & 0 \end{bmatrix}$, $Q = \begin{bmatrix} 1 \\ 0 \end{bmatrix}$, $b_l = 0$ and $b_i = 1$ if $i \neq l$, $a_{ij}(t)$ is defined as: $a_{ij}(t) = 1$ if $(j, i) \in \mathcal{E}_c(t)$; $a_{ij}(t) = 0$, otherwise. Moreover, $\mu_i, \nu_i > 0$ and the initial states $\hat{\boldsymbol{q}}_0^i(t_0)$ and $\hat{\omega}_i(t_0)$ are properly selected such that $\bar{v}_i(t_0) = v_i(t_0)$ and $\bar{\omega}_i(t_0) = \omega_i(t_0)$. That is, $\mu_i, \nu_i > 0$, $\hat{\boldsymbol{q}}_0^i(t_0)$ and $\hat{\omega}_i(t_0)$ are chosen as

$$\hat{\omega}_i(t_0) = v_i(t_0)/r - k_1\tanh(k_2b_i\sum_{j\in\mathcal{N}_s^i(t_0)}(\theta_j^i(t_0) - \alpha_{ji})), \tag{17}$$

$$Q^{\mathrm{T}}\hat{\boldsymbol{q}}_0^i(t_0) = \frac{\operatorname{arctanh}((v_i(t_0) - \omega_i(t_0)r)/\mu_i)}{\nu_i}. \tag{18}$$

In addition, the initial $\check{\boldsymbol{q}}_0^l(t_0)$ is set to $\check{\boldsymbol{q}}_0^l(t_0) = \boldsymbol{q}_0^l(t_0)$ since $\boldsymbol{q}_0^l(t_0)$ is known under Assumption 3.

The proposed control law (9)–(14) is in the form of (2)–(3). Torque F_i in (9) is for achieving the desired spacing along the common circle, and torque T_i in (10) is for achieving the convergence to the common circle with center $\boldsymbol{q}_0$. To implement control law (9)–(14), the sensors of unicycle i need to measure the relative states $\boldsymbol{p}_j^i$ and θ_j^i. The communication device of unicycle i is used to receive the information $\hat{\boldsymbol{q}}_0^j$ from its neighbors.

The main theorem of this paper is stated as follows.

Theorem 1 The *circular formation control problem*, i.e., Problem 1, can be solved by the dynamic control law (9)–(14) with (15)–(16) under Assumptions 1–4. ■

In fact, $[F_i\ T_i]^{\mathrm{T}}$ in (9)–(10) is designed such that $I\dot{\bar{v}}_i = F_i$ and $J\dot{\bar{\omega}}_i = T_i$, equivalently, $\dot{v}_i - \dot{\bar{v}}_i = 0,\ \dot{\omega}_i - \dot{\bar{\omega}}_i = 0$. Since $[\bar{v}_i(t_0)\ \bar{\omega}_i(t_0)]^{\mathrm{T}}$ is set to $[v_i(t_0)\ \omega_i(t_0)]^{\mathrm{T}}$, we have

$$v_i(t) = \bar{v}_i(t),\ \omega_i(t) = \bar{\omega}_i(t),\ \forall t \geq t_0. \tag{19}$$

Thus, the dynamic unicycle i in the form of (1) is reduced to a kinematic unicycle in the following form

$$\dot{x}_i = \bar{v}_i\cos\theta_i,\ \dot{y}_i = \bar{v}_i\sin\theta_i,\ \dot{\theta}_i = \bar{\omega}_i, \tag{20}$$

with $\bar{v}_i$ and $\bar{\omega}_i$ being the control inputs. Using (8) and (19), the dynamics of the tracking errors $\boldsymbol{p}_{ei}$ become

$$\dot{\boldsymbol{p}}_{ei} = \bar{\omega}_i S \boldsymbol{p}_{ei} + (\bar{\omega}_i r - \bar{v}_i)Q. \quad (21)$$

Moreover, since $\dot{\boldsymbol{q}}_0^l = \omega_l S \boldsymbol{q}_0^l - v_l Q$, it follows from (13), (19), and $\check{\boldsymbol{q}}_0^l(t_0) = \boldsymbol{q}_0^l(t_0)$ that $\check{\boldsymbol{q}}_0^l(t) = \boldsymbol{q}_0^l(t), \forall t \geq t_0$, which makes $\boldsymbol{q}_0^l(t)$ known to unicycle l.

Hence, to prove Theorem 1, it suffices to show that the kinematic unicycles (20) with controller $[\bar{v}_i\ \bar{\omega}_i]^{\mathrm{T}}$ in (15)–(16) can achieve the global convergence to the common circle and the desired spacing. To this end, Theorem 1 is proved by the following two steps.

Step 1: Show the global convergence to the common circle. That is, consider the closed-loop system consisting of (11)–(16) and N systems (21), and prove that $x_{ei}(t)$ converges to zero, $y_{ei}(t)$ converges to zero if $\bar{v}_i(t)$ does not converge to zero, and $\bar{\omega}_i(t)$ converges to $\bar{v}_i(t)/r$.

Step 2: Show the global convergence to the desired spaced formation. That is, consider the closed-loop system consisting of (11)–(16) and N systems $\dot{\theta}_i = \bar{\omega}_i$, and prove that $\boldsymbol{\theta}$ converges to set $\mathcal{S}$ and $\bar{v}_i(t)$ converge to ϖr.

Remark 3 If the initial velocity measurements were impacted by noises, (19) would not hold. To avoid this situation in practice, each unicycle may start with static state, i.e., $v_i(t_0) = \omega_i(t_0) = 0$. Thus, the initial velocities measurements are not needed any longer. Note that each unicycle can choose its own initial time. Moreover, once $\hat{\omega}_i(t_0)$, k_1, and μ_i are determined, v_i and ω_i are maintained within known bounds for all time. ■

3.1 Step 1: Global Convergence to the Common Circle

In this subsection, we show that all kinematic unicycles (20) globally converge to a common circle with center $\boldsymbol{q}_0$ and radius r, provided that $\bar{v}_i(t)$ does not converge to zero. To this end, the following proposition is needed.

Proposition 1 Consider N subsystems in the form of (11)–(13) with the communication graph $\mathcal{G}_c$. Given a center $\boldsymbol{q}_0 \in \mathbb{R}^2$ and a radius r, under Assumptions 1–3, for any initial states $\hat{\boldsymbol{q}}_0^i(t_0) \in \mathbb{R}^2$, $\forall t_0 \geq 0$, $i = 1, ..., N$, $\hat{\boldsymbol{q}}_0^i(t)$ converge to $\boldsymbol{q}_0^i(t)$ *exponentially* as $t \to \infty$. ■

Proof: Define $\tilde{\boldsymbol{q}}_i = \hat{\boldsymbol{q}}_0^i - \boldsymbol{q}_0^i$. Using (11), (12), (13), (19), and $\check{\boldsymbol{q}}_0^l(t) = \boldsymbol{q}_0^l(t), \forall t \geq t_0$ yields

$$\dot{\tilde{\boldsymbol{q}}}_i = \bar{\omega}_i S \tilde{\boldsymbol{q}}_i + k_3(-b_i \tilde{\boldsymbol{q}}_i + \sum_{j \in \mathcal{N}_c^i(t)} a_{ij}(t)(R(\theta_i^j)\tilde{\boldsymbol{q}}_j - \tilde{\boldsymbol{q}}_i)), \quad (22)$$

where $b_l = 1$, $a_{lj}(t) = 0$ and $b_i = 0$ if $i \neq l$.

Consider a Lyapunov function candidate $V_i(\tilde{\boldsymbol{q}}_i) = \frac{1}{2}\tilde{\boldsymbol{q}}_i^{\mathrm{T}}\tilde{\boldsymbol{q}}_i$. Taking its time derivative along the trajectories of system (22) leads to

$$\begin{aligned}\dot{V}_i(\tilde{\boldsymbol{q}}_i) &= \frac{1}{2}\tilde{\boldsymbol{q}}_i^{\mathrm{T}}(S + S^{\mathrm{T}})\tilde{\boldsymbol{q}}_i - k_3(b_i \tilde{\boldsymbol{q}}_i^{\mathrm{T}}\tilde{\boldsymbol{q}}_i + \sum_{j \in \mathcal{N}_c^i(t)} a_{ij}(t)\tilde{\boldsymbol{q}}_i^{\mathrm{T}}\tilde{\boldsymbol{q}}_i \\ &\quad - \sum_{j \in \mathcal{N}_c^i(t)} a_{ij}(t)\frac{1}{2}(\tilde{\boldsymbol{q}}_i^{\mathrm{T}} R(\theta_i^j)\tilde{\boldsymbol{q}}_j + \tilde{\boldsymbol{q}}_j^{\mathrm{T}} R^{\mathrm{T}}(\theta_i^j)\tilde{\boldsymbol{q}}_i)) \\ &\leq k_3(-b_i\|\tilde{\boldsymbol{q}}_i\|^2 + \sum_{j \in \mathcal{N}_c^i(t)} a_{ij}(t)(\|\tilde{\boldsymbol{q}}_j\|\|\tilde{\boldsymbol{q}}_i\| - \|\tilde{\boldsymbol{q}}_i\|^2)),\end{aligned}$$

where it is noted that $S + S^{\mathrm{T}} = 0$ and $\|R(\theta_i^j)\tilde{\boldsymbol{q}}_j\| = \|\tilde{\boldsymbol{q}}_j\|$. Define $\bar{q}_i = \|\tilde{\boldsymbol{q}}_i\|$. Using $V_i(\tilde{\boldsymbol{q}}_i) = \frac{1}{2}\|\tilde{\boldsymbol{q}}_i\|^2 = \frac{1}{2}\bar{q}_i^2$, the right-hand time derivative of $\bar{q}_i$ satisfies

$$\mathrm{D}^+ \bar{q}_i \leq k_3(-b_i \bar{q}_i + \sum_{j \in \mathcal{N}_c^i(t)} a_{ij}(t)(\bar{q}_j - \bar{q}_i)). \quad (23)$$

Denote $\bar{\boldsymbol{q}} = [\bar{q}_1, ..., \bar{q}_N]^{\mathrm{T}}$, and N inequalities in the form of (23) are rewritten in the following compact form

$$\mathrm{D}^+ \bar{\boldsymbol{q}} \leq -\mathcal{H}(t)\bar{\boldsymbol{q}}, \quad (24)$$

where $\mathcal{H}(t)$ is a block matrix of the Laplacian matrix $\bar{\mathcal{L}}_c(t)$ of a digraph $\bar{\mathcal{G}}_c(t)$ obtained by firstly removing all directed edges (j, l), $j \in \mathcal{N}_c^i(t)$, in digraph $\mathcal{G}_c(t)$, and then adding node 0 (denoting $\boldsymbol{q}_0$) and a directed edge $(0, l)$. Thus, $\bar{\mathcal{L}}_c(t)$ can be partitioned as $\bar{\mathcal{L}}_c(t) = \left(\begin{array}{c|c} 0 & [0, ..., 0] \\ \hline -\mathcal{A}_0(t)\mathbf{1} & \mathcal{H}(t)\end{array}\right)$, where $\mathcal{A}_0(t) = \mathrm{diag}$ $(a_{10}(t), ..., a_{N0}(t))$. If $\mathcal{G}_c(t) = \mathcal{G}$, $\forall t \geq t_0$, then $\bar{\mathcal{G}}(t) = \bar{\mathcal{G}}$, where $\bar{\mathcal{G}}$ is fixed and contains a directed spanning tree with node 0 being the root by Assumptions 1 and 3.

It follows from Lemma 3 and (24) that

$$\bar{\boldsymbol{q}}(t) \leq e^{-\mathcal{H}(t-t')}\bar{\boldsymbol{q}}(t'),\ \forall t \geq t' \geq t_0. \quad (25)$$

Then, consider an instant $t_n^k > t_0$, $n \geq 1$, and we have

$$\begin{aligned}\bar{\boldsymbol{q}}(t_n^k) &\leq e^{-\mathcal{H}(t_n^{k-1})(t_n^k - t_n^{k-1})}\bar{\boldsymbol{q}}(t_n^{k-1}) \\ &= e^{-\mathcal{H}(t_n^{k-1})(t_n^k - t_n^{k-1}) - ... - \mathcal{H}(t_0^0)(t_0^1 - t_0^0)}\bar{\boldsymbol{q}}(t_0) \\ &\leq e^{-\mathcal{H}(t_n^{k-1})\bar{\tau} - ... - \mathcal{H}(t_0^0)\bar{\tau}}\bar{\boldsymbol{q}}(t_0) \\ &\leq e^{-\sum_{m=0}^{n}\sum_{k=0}^{k_m}\mathcal{H}(t_m^k)\bar{\tau}}\bar{\boldsymbol{q}}(t_0),\end{aligned} \quad (26)$$

since $t_n^{k+1} - t_n^k \geq \bar{\tau} > 0$. Let $H(t_m) = \sum_{k=0}^{k_m} c_m^k \mathcal{H}(t_m^k)$. Under Assumption 2, $\bigcup_{j=0}^{j=k_m-1}\mathcal{G}_c(t_m^j) = \mathcal{G}$ during each time subinterval $[t_m^k, t_m^{k+1})$, $k = 0, 1, ..., k_m - 1$.

Define $\bar{\mathcal{L}}(t_m)$ as the Laplacian matrix of a graph $\bar{\mathcal{G}}(t_m)$ which is an edge-weighted graph of $\bar{\mathcal{G}}$. Similarly, $H(t_m)$ is a block matrix of $\bar{\mathcal{L}}(t_m)$, i.e, $\bar{\mathcal{L}}(t_m) = \left(\begin{array}{c|c} 0 & [0, ..., 0] \\ \hline -\mathcal{A}_0(t_m)\mathbf{1} & H(t_m)\end{array}\right)$. Using Lemma 1 in Su & Huang

(2012), all eigenvalues of $H(t_m)$ have positive real parts. Thus, the minimum real part of these eigenvalues, i.e., $\underline{\lambda}(H(t_m))$, is positive. By (26), we have $\|\bar{\boldsymbol{q}}(t_n^k)\| \leq \|e^{-\bar{\tau}\sum_{m=0}^{n} H(t_m^k)}\bar{\boldsymbol{q}}(t_0)\| \leq e^{-\bar{\tau}\sum_{m=0}^{n}\underline{\lambda}(H(t_m^k))}\|\bar{\boldsymbol{q}}(t_0)\|$. Since $n \to \infty$ as $t \to \infty$, $\bar{\boldsymbol{q}}(t)$ converges to $\mathbf{0}$ exponentially as $t \to \infty$. This completes the proof. ■

Next, the following proposition can be obtained.

Proposition 2 Consider N systems (21) with the communication graph $\mathcal{G}_c$, and control law (11)–(16). Under Assumptions 1–3, for any initial states $\boldsymbol{p}_{ei}(t_0) \in \mathbb{R}^2$, $i = 1, ..., N$, $\forall t_0 \geq 0$, $x_{ei}(t)$ converges to zero asymptotically as $t \to \infty$, $y_{ei}(t)$ converges to zero if $\bar{v}_i(t)$ does not converge to zero, and $\bar{\omega}_i(t)$ converges to $\bar{v}_i(t)/r$. ■

Proof: Define $\hat{\boldsymbol{p}}_{ei} := [\hat{x}_{ei}\ \hat{y}_{ei}]^{\mathrm{T}}$ as $\hat{\boldsymbol{p}}_{ei} = \hat{\boldsymbol{q}}_0^i + rP$, and $\tilde{\boldsymbol{p}}_{ei} := [\tilde{x}_{ei}\ \tilde{y}_{ei}]^{\mathrm{T}}$ as $\tilde{\boldsymbol{p}}_{ei} = \hat{\boldsymbol{p}}_{ei} - \boldsymbol{p}_{ei}$. By (8), we have

$$\tilde{\boldsymbol{p}}_{ei} = \hat{\boldsymbol{q}}_0^i - \boldsymbol{q}_0^i = \tilde{\boldsymbol{q}}_i. \tag{27}$$

Then, the closed-loop system consisting of (21) and the dynamic control law (11)–(16), can be written as

$$\dot{\boldsymbol{p}}_{ei} = \boldsymbol{f}(\boldsymbol{p}_{ei}, \bar{\omega}_i(t)) + \boldsymbol{g}(\boldsymbol{p}_{ei}, \tilde{\boldsymbol{p}}_{ei}, \bar{\omega}_i(t)), \tag{28}$$

where $\boldsymbol{f}(\boldsymbol{p}_{ei}, \bar{\omega}_i(t)) = \bar{\omega}_i S \boldsymbol{p}_{ei} + (\omega_{ei} r - \bar{v}_i)Q$, and $\boldsymbol{g}(\boldsymbol{p}_{ei}, \tilde{\boldsymbol{p}}_{ei}, \bar{\omega}_i(t)) = (\bar{\omega}_i - \omega_{ei})Q$ with $\omega_{ei} = \bar{v}_i/r - \mu_i \tanh(\nu_i Q^{\mathrm{T}}(\boldsymbol{q}_i^i + rP))/r$. Moreover, $|\bar{\omega}_i - \omega_{ei}|$ satisfies

$$\begin{aligned} |\bar{\omega}_i - \omega_{ei}| &= \mu_i |(\tanh(\nu_i(x_{ei} + \tilde{x}_{ei})) - \tanh(\nu_i x_{ei}))|/r \\ &\leq \mu_i \varsigma |\tilde{x}_{ei}|/r, \end{aligned} \tag{29}$$

with some constant $\varsigma > 0$. System (28) can be considered as the nominal system $\dot{\boldsymbol{p}}_{ei} = \boldsymbol{f}(\boldsymbol{p}_{ei}, \bar{\omega}_i(t))$ with a perturbation. By (14), $\hat{\omega}_i(t)$ converges to ϖ exponentially as $t \to \infty$. By (15) and (16), $\bar{\omega}_i$ is uniformly bounded. It follows from Proposition 1, (27) and (29) that $\|\boldsymbol{g}(\boldsymbol{p}_{ei}, \tilde{\boldsymbol{p}}_{ei}, \bar{\omega}_i(t))\|$ converges to zero exponentially as $t \to \infty$. Then, the remaining proof to show that $x_{ei}(t)$ converges to zero asymptotically and $y_{ei}(t)$ converges to zero if $\bar{v}_i(t)$ does not converge to zero, can be done by mimicking the proof of Lemma 3.3 in Yu & Liu (2016a). As $x_{ei}(t)$ converges to zero, $\bar{\omega}_i(t)$ converges to $\bar{v}_i(t)/r$. ■

3.2 *Step 2: Global Convergence to a Desired Spacing*

In this subsection, we show that that all kinematic unicycles (20) achieve the desired spacing along the common circle, as is summarized in the following proposition.

Proposition 3 Consider the sensor graph $\mathcal{G}_s$ under Assumptions 1–2, and systems $\dot{\theta}_i = \bar{\omega}_i,\ i = 1, ..., N$, with control law (11)–(16). For any initial states $\boldsymbol{\theta}(t_0) \in \mathbb{R}^N$, $\forall t_0 \geq 0$, $\boldsymbol{\theta}(t)$ converges to set $\mathcal{S}$ asymptotically as $t \to \infty$, and meanwhile $\bar{v}_i(t)$ converges to ϖr. ■

Proof: Define $\phi_i = k_2 b_i \sum_{j\in\mathcal{N}_s^i(t)} (\theta_j^i - \alpha_{ji})$, and it follows from (15) and (16) that

$$\dot{\phi}_i = k_2 b_i \sum_{j\in\mathcal{N}_s^i(t)} (k_1(\tanh\phi_j - \tanh\phi_i) + \varepsilon_j - \varepsilon_i), \tag{30}$$

where $\varepsilon_i = \hat{\omega}_i - \mu_i \tanh(\nu_i Q^{\mathrm{T}} \hat{\boldsymbol{q}}_0^i)/r$.

Define $\gamma_i = \tanh\phi_i$ and $\gamma_i \in (-1\ 1)$. With denoting $\boldsymbol{\gamma} = [\gamma_1, ..., \gamma_N]^{\mathrm{T}}$ and $\boldsymbol{\varepsilon} = [\varepsilon_1, ..., \varepsilon_N]^{\mathrm{T}}$, the dynamics of $\boldsymbol{\gamma}$ can be written in the following compact form

$$\dot{\boldsymbol{\gamma}} = -k_1 k_2 W(\boldsymbol{\gamma})\mathcal{L}\boldsymbol{\gamma} - k_2 W(\boldsymbol{\gamma})\mathcal{L}\boldsymbol{\varepsilon}, \tag{31}$$

where it is noted that $\mathcal{L}_s(t) = \mathcal{L}$ by Assumption 2, and $W(\boldsymbol{\gamma}) = \mathrm{diag}(b_1(1-\gamma_1^2), ..., b_N(1-\gamma_N^2))$. System (31) can be viewed as the following nominal system

$$\dot{\boldsymbol{\gamma}} = -k_1 k_2 W(\boldsymbol{\gamma})\mathcal{L}\boldsymbol{\gamma}, \tag{32}$$

with perturbation $-k_2 W(\boldsymbol{\gamma})\mathcal{L}\boldsymbol{\varepsilon}$. First, we show that the nominal system (32) is exponentially stable at $\boldsymbol{\gamma} = \mathbf{0}$.

Under Assumption 1, let node 1 denote the root node, i.e., $l = 1$. Define $\tilde{\gamma}_i = \gamma_i - \gamma_1$, $i \geq 2$, and denote $\tilde{\boldsymbol{\gamma}} = [\tilde{\gamma}_2, ..., \tilde{\gamma}_N]^{\mathrm{T}}$. Since $b_1 = 0$ and $b_i = 1$ if $i \neq l$, then $\phi_1 = 0$, $\dot{\phi}_1 = 0$, $\gamma_1 = 0$, and $\dot{\gamma}_1 = 0$. It follows from (32) that the dynamics of $\tilde{\boldsymbol{\gamma}}$ can be written as

$$\dot{\tilde{\boldsymbol{\gamma}}} = -k_1 k_2 \underline{W}(\tilde{\boldsymbol{\gamma}})(\underline{\mathcal{L}} + \underline{\mathcal{A}})\tilde{\boldsymbol{\gamma}}, \tag{33}$$

where $\underline{W}(\tilde{\boldsymbol{\gamma}}) = \mathrm{diag}(1-\tilde{\gamma}_2^2, ..., 1-\tilde{\gamma}_N^2)$, $\underline{\mathcal{L}}$ is the Laplacian matrix of a graph $\underline{\mathcal{G}}$ obtained by removing node 1 and edges $(1, i)$, $(i, 1)$, $i \geq 2$, from $\mathcal{G}$, and $\underline{\mathcal{A}} = \mathrm{diag}(a_{21}, ..., a_{N1})$ with $a_{i1} = 1$ for $(1, i) \in \mathcal{E}$ and $a_{i1} = 0$ for $(1, i) \notin \mathcal{E}$. Since $\gamma_i \in (-1, 1)$, $\underline{W}(\tilde{\boldsymbol{\gamma}})$ is always positive definite.

Define $U = \mathrm{diag}(u_2, ..., u_N)$ with $u_i = \zeta_i/\eta_i$, $i \geq 2$, $\boldsymbol{\eta} = [\eta_2, ..., \eta_N]^{\mathrm{T}} = (\underline{\mathcal{L}} + \underline{\mathcal{A}})\mathbf{1}$, $\boldsymbol{\zeta} = [\zeta_2, ..., \zeta_N]^{\mathrm{T}} = (\underline{\mathcal{L}} + \underline{\mathcal{A}})^{-\mathrm{T}}\mathbf{1}$. By Lemma 2, U is positive definite. Furthermore, define $D(\boldsymbol{\gamma}) = \mathrm{diag}(d_2, ..., d_N)$ with $d_i = d(\gamma_i)$, $i \geq 2$, where $d(\cdot) : (-1, 1) \to \mathbb{R}$ is defined as $d(x) = 1$ if $x = 0$; $d(x) = \frac{1}{x^2}h(x)$ if $x \in (-1, 1) \setminus \{0\}$, with $h(\cdot) : (-1, 1) \to \mathbb{R}$ satisfying $\frac{\partial h(x)}{\partial x} = \frac{2x}{1-x^2}$. By L'Hospital's rule, $\lim_{x\to 0} d(x) = 1 = d(0)$, and $d(x)$ is a differentiable function satisfying

$$d(x)(1-x^2) + \frac{1}{2}\frac{\partial d(x)}{\partial x}x(1-x^2) = 1. \tag{34}$$

By (34), it can be verified that $d(x) > 0$ for $x \in (-1, 1)$.

Consider the following Lyapunov function candidate $V(\tilde{\boldsymbol{\gamma}}) = \frac{1}{2}\tilde{\boldsymbol{\gamma}}^{\mathrm{T}} U D \tilde{\boldsymbol{\gamma}}$. Taking its time derivative along the trajectories of the nominal system (32) yields

$$\begin{aligned} \dot{V}(\tilde{\boldsymbol{\gamma}}) &= -k_1 k_2 \tilde{\boldsymbol{\gamma}}^{\mathrm{T}}(UD\underline{W}(\underline{\mathcal{L}} + \underline{\mathcal{A}}) + (\underline{\mathcal{L}} + \underline{\mathcal{A}})^{\mathrm{T}}\underline{W}UD)\tilde{\boldsymbol{\gamma}} \\ &\quad + \sum_{i=2}^{N}(u_i\tilde{\gamma}_i^2\frac{\partial d_i}{\partial\tilde{\gamma}_i}(1-\tilde{\gamma}_i^2)\sum_{j\in\mathcal{N}_i}(\tilde{\gamma}_j - \tilde{\gamma}_i)), \\ &= -k_1 k_2 \tilde{\boldsymbol{\gamma}}^{\mathrm{T}}(U\underline{D}(\underline{\mathcal{L}} + \underline{\mathcal{A}}) + (\underline{\mathcal{L}} + \underline{\mathcal{A}})^{\mathrm{T}}U\underline{D})\tilde{\boldsymbol{\gamma}}, \end{aligned} \tag{35}$$

where $\underline{D} = D(\tilde{\gamma})\underline{W}(\tilde{\gamma}) - \frac{1}{2}\frac{\partial D(\tilde{\gamma})}{\partial \tilde{\gamma}}\underline{W}(\tilde{\gamma})\mathrm{diag}(\tilde{\gamma}_2, ..., \tilde{\gamma}_N)$. Thus, $\underline{D} = \mathrm{diag}(\underline{d}_2, ..., \underline{d}_N)$ is a diagonal matrix with $\underline{d}_i = d_i(1-\tilde{\gamma}_i^2) + \frac{\partial d_i}{2\partial \tilde{\gamma}_i}\tilde{\gamma}_i(1-\tilde{\gamma}_i^2)$, $i \geq 2$. Then, it follows from (34) that $\underline{d}_i = 1$, $\underline{D} = I_{N-1}$, and

$$\dot{V}(\tilde{\gamma}) = -k_1 k_2 \tilde{\gamma}^{\mathrm{T}}(U(\underline{\mathcal{L}}+\underline{\mathcal{A}}) + (\underline{\mathcal{L}}+\underline{\mathcal{A}})^{\mathrm{T}}U)\tilde{\gamma}. \quad (36)$$

By Assumption 1 and Lemma 2, $U(\underline{\mathcal{L}}+\underline{\mathcal{A}}) + (\underline{\mathcal{L}}+\underline{\mathcal{A}})^{\mathrm{T}}U$ is positive definite. It follows from (35) that $\dot{V}(\tilde{\gamma}) \leq 0$ and $\tilde{\boldsymbol{\gamma}} = \mathbf{0}$ of system (33) is asymptotically stable for all $\tilde{\boldsymbol{\gamma}} \in (-1, 1)$. Since $\gamma_1 = 0$, each $\gamma_i(t)$ converges to 0 as $t \to \infty$, and $\boldsymbol{\gamma} = \mathbf{0}$ of system (32) is asymptotically stable all $\boldsymbol{\gamma} \in (-1, 1)$.

We then show that the perturbation term $-W(\boldsymbol{\gamma})\mathcal{L}\boldsymbol{\varepsilon}$ with $\varepsilon_i = \hat{\omega}_i - \mu_i \tanh(\nu_i Q^{\mathrm{T}}\hat{\boldsymbol{q}}_0^i)/r$ converges to zero exponentially. By (14), $\hat{\omega}_i(t)$ exponentially converges to ϖ as $t \to \infty$. By Proposition 1, $Q^{\mathrm{T}}\hat{\boldsymbol{q}}_0^i(t)$ exponentially converges to $Q^{\mathrm{T}}\boldsymbol{q}_0^i(t)$, and by (8) and Proposition 2, $Q^{\mathrm{T}}\boldsymbol{q}_0^i(t) = x_{ei}(t)$ asymptotically converges to zero. Thus, $\varepsilon_i(t)$ asymptotically converges to ϖ and $-\mathcal{L}\boldsymbol{\varepsilon}(t)$ asymptotically converges to zero as $t \to \infty$.

Recall the nominal system of system (28), i.e., $\dot{\boldsymbol{p}}_{ei} = \bar{\omega}_i S p_{ei} - (\mu_i \tanh(\nu_i x_{ei}))Q$, which can be rewritten as

$$\dot{\boldsymbol{p}}_{ei} = A_i(t)\boldsymbol{p}_{ei} + \epsilon_i(t)\boldsymbol{p}_{ei}, \quad (37)$$

$$A_i(t) = \begin{bmatrix} -\mu_i\nu_i & \bar{\omega}_i \\ -\bar{\omega}_i & 0 \end{bmatrix}, \; \epsilon_i(t) = \mu_i\nu_i \begin{bmatrix} 1 - \frac{\tanh(\nu_i x_{ei})}{\nu_i x_{ei}} & 0 \\ 0 & 0 \end{bmatrix}.$$

Note that $\bar{\omega}_i$ is persistently exciting if $\bar{v}_i$ does not converge to 0. Suppose that $\bar{v}_i(t)$ converges to 0. It follows from (14) and (15) that γ_i converges to $-\varpi/k_1$. It follows from (31) and $-\mathcal{L}\boldsymbol{\varepsilon} \to 0$ that $\dot{\boldsymbol{\gamma}}$ does not converge to zero, which yields a contradiction. Then, by Lemma 1, $\boldsymbol{p}_{ei} = \mathbf{0}$ of the system $\dot{\boldsymbol{p}}_{ei} = A_i(t)\boldsymbol{p}_{ei}$ is globally exponentially stable.

Moreover, $x_{ei}(t)$ converges to 0 by Proposition (2), and $1 - \frac{\tanh(\nu_i x_{ei})}{\nu_i x_{ei}}$ converges to 0 as $x_{ei} \to 0$ by L'Hospital's rule. Then, it follows from Khalil (2002, Corollary 9.1 and Lemma 9.5) that $\boldsymbol{p}_{ei} = \mathbf{0}$ of system (37) is globally exponentially stable. Thus, $-\mathcal{L}\boldsymbol{\varepsilon}(t)$ exponentially converges to zero as $t \to \infty$

Hence, by Yu & Liu (2016b, Lemma 2.1), $\boldsymbol{\gamma}(t)$ converges to zero asymptotically as $t \to \infty$, i.e., $\lim_{t\to\infty} \boldsymbol{\phi}(t) = \mathbf{0}$. Noting that $\boldsymbol{\phi} = \mathcal{L}_s(\boldsymbol{\theta} - \boldsymbol{\alpha})$, then $\lim_{t\to\infty} \mathcal{L}_s(\boldsymbol{\theta}(t) - \boldsymbol{\alpha}) = \mathbf{0}$. Moreover, it can be checked from (15) that $\lim_{t\to\infty} \bar{v}_i(t) = \varpi r$. This completes the proof. ∎

With Propositions 1–3, the proof of Theorem 1 can be summarized as follows.

Proof of Theorem 1: First, by Proposition 2 and $\lim_{t\to\infty} \bar{v}_i(t) = \varpi r > 0$ in Proposition 3, each $\boldsymbol{p}_{ei}(t)$ converges to zero asymptotically as $t \to \infty$. Then, Proposition 3 shows that $\boldsymbol{\theta}(t)$ converges to set $\mathcal{S}$ asymptotically as $t \to \infty$. Finally, it follows from (16), $\lim_{t\to\infty} \bar{v}_i(t) = \varpi r$, Propositions 1 and 2 that $\lim_{t\to\infty} \bar{\omega}_i(t) = \varpi$. ∎

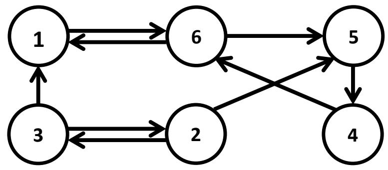

Fig. 1. The topology of digraph $\mathcal{G}$.

4 An Illustrative Example

Consider 6 dynamic unicycles (1) with digraph $\mathcal{G}$ shown in Fig. 1, the sensor graph $\mathcal{G}_s(t) = \mathcal{G}$, and the communication graph $\mathcal{G}_c(t) = \{\mathcal{O}, \mathcal{E}_c(t)\}$, where $\mathcal{E}_c(t) = \{(3,1),(6,1)\}$ if $s\bar{T} \leq t < (s+0.3)\bar{T}$, $\mathcal{E}_c(t) = \{(2,3),(5,4)\}$ if $(s+0.3)\bar{T} \leq t < (s+0.5)\bar{T}$, $\mathcal{E}_c(t) = \{(6,5),(2,5)\}$ if $(s+0.5)\bar{T} \leq t < (s+0.7)\bar{T}$, and $\mathcal{E}_c(t) = \{(1,6),(4,6)\}$ if $(s+0.7)\bar{T} \leq t < (s+1)\bar{T}$, $s = 0, 1, 2...$, $\bar{T} = 6$s. Set $l = 2$. Thus, Assumptions 1–3 are satisfied. Assume $I = J = 1$, and let $r = \varpi = 1$.

The center $\boldsymbol{q}_0$ is set to $[1.2\ 1.8]^{\mathrm{T}}$. The initial states of unicycles are $\theta_1(0) = 0.5\pi$, $\theta_2(0) = 0$, $\theta_3(0) = 0.5\pi$, $\theta_4(0) = \pi$, $\theta_5(0) = 1.5\pi$, $\theta_6(0) = 0$, $\boldsymbol{p}_1(0) = [-1\ 1.3]^{\mathrm{T}}$, $\boldsymbol{p}_2(0) = [2\ 1.5]^{\mathrm{T}}$, $\boldsymbol{p}_3(0) = [1.5\ 1.6]^{\mathrm{T}}$, $\boldsymbol{p}_4(0) = [1.6\ -1.6]^{\mathrm{T}}$, $\boldsymbol{p}_5(0) = [1\ \ -1.5]^{\mathrm{T}}$, $\boldsymbol{p}_6(0) = [-1\ -0.2]^{\mathrm{T}}$, $v_1(0) = 1$, $v_2(0) = 2$, $v_3(0) = 1.5$, $v_4(0) = 0.6$, $v_5(0) = 0.5$, $v_6(0) = 1.2$, $\omega_1(0) = 0.8$, $\omega_2(0) = 1.2$, $\omega_3(0) = 1.3$, $\omega_4(0) = 0.9$, $\omega_5(0) = 1.1$, and $\omega_6(0) = 0.7$.

Set $k_1 = k_2 = k_4 = 1$, $k_3 = 10$, $\mu_i = 2$, and $\nu_i = 1$, $i = 1, ..., 6$. According to (17)–(18), we obtain $\hat{\omega}_1(0) = 1.9701$, $\hat{\omega}_2(0) = 1.5195$, $\hat{\omega}_3(0) = 1.9805$, $\hat{\omega}_4(0) = 0.1195$, $\hat{\omega}_5(0) = 1.5$, $\hat{\omega}_6(0) = 0.2$, $\hat{\boldsymbol{q}}_0^1(0) = [0.1003\ \ -0.1623]^{\mathrm{T}}$, $\hat{\boldsymbol{q}}_0^2(0) = [0.4236\ 0.4001]^{\mathrm{T}}$, $\hat{\boldsymbol{q}}_0^3(0) = [0.1003\ -0.1308]^{\mathrm{T}}$, $\hat{\boldsymbol{q}}_0^4(0) = [-0.1511\ -0.3888]^{\mathrm{T}}$, $\hat{\boldsymbol{q}}_0^5(0) = [-0.3095\ 0.2803]^{\mathrm{T}}$, and $\hat{\boldsymbol{q}}_0^6(0) = [0.2554\ \ -0.1103]^{\mathrm{T}}$.

When the desired spacing is $\boldsymbol{\alpha} = [0\ \frac{\pi}{3}\ \frac{2\pi}{3}\ \pi\ \frac{4\pi}{3}\ \frac{5\pi}{3}]$, the trajectories of all unicycles during 0–100s are presented in Fig. 2, which shows that all unicycles converge to the desired circular formation. Fig. 3 shows that the relative distance between each unicycle and the center $\boldsymbol{q}_0$ converges to r, and Fig. 4 illustrates that the unicycles converges to the desired spaced formation. When the desired spacing $\boldsymbol{\alpha}$ is changed to $\boldsymbol{\alpha}' = [0\ \frac{\pi}{6}\ \frac{\pi}{3}\ \frac{\pi}{2}\ \frac{2\pi}{3}\ \frac{5\pi}{6}]$, the trajectories of all unicycles during 0–100s is shown in Fig. 5. These simulation results verify the effectiveness of the proposed control law.

5 Conclusion

In this paper, a distributed dynamic control law is proposed for networked dynamic unicycles, such that unicycles can globally converge to a circular formation with a desired spacing along the circle. The topology of the network is modeled by a directed graph, and center is only known to one unicycle. For future work, we will study the formation control of networked unicycles under proximity graph and consider the collision avoidance.

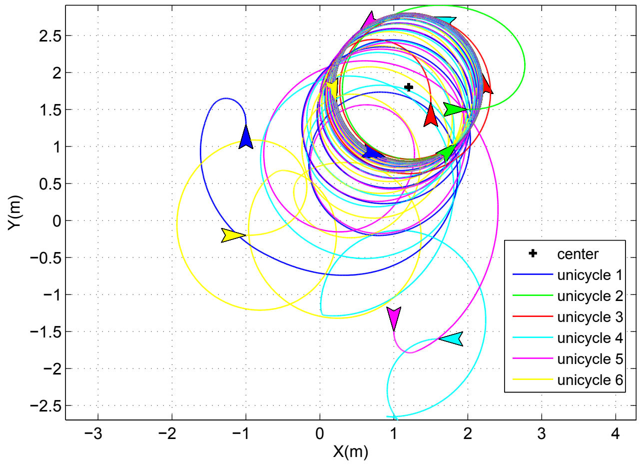

Fig. 2. Trajectories of unicycles with the desired spacing $\boldsymbol{\alpha}$.

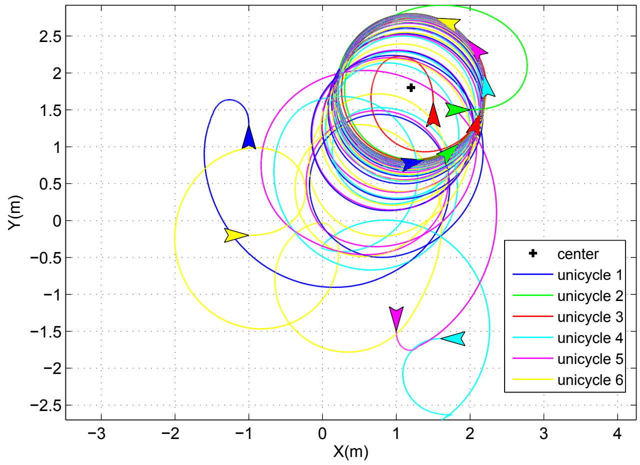

Fig. 5. Trajectories of unicycles with the desired spacing $\boldsymbol{\alpha}'$.

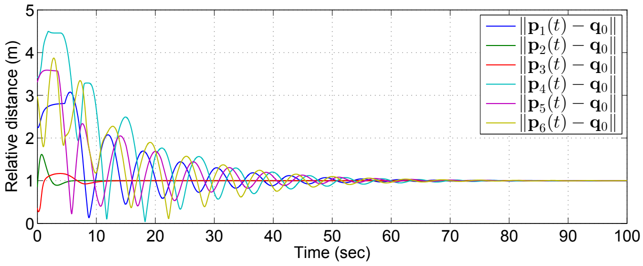

Fig. 3. Relative distances $\|\boldsymbol{p}_i - \boldsymbol{q}_0\|$, $i = 1, ..., 6$.

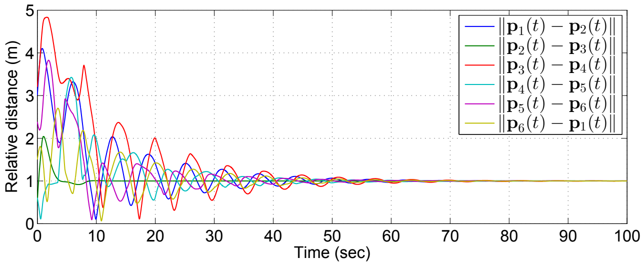

Fig. 4. Relative distances $\|\boldsymbol{p}_i(t) - \boldsymbol{p}_{(i+1)}(t)\|$, $i = 1, ..., 5$, and $\|\boldsymbol{p}_6(t) - \boldsymbol{p}_1(t)\|$.

Appendix Proof of Lemma 3

To prove Lemma 3, we only need to prove that for any $t_1 < T$, $\boldsymbol{x}(t) \le \boldsymbol{y}(t)$, $\forall t \in [t_0, t_1]$. Consider the following vectorial differential equation

$$\dot{\boldsymbol{z}} = \boldsymbol{f}(t, \boldsymbol{z}) + \lambda \mathbf{1},\ \ \boldsymbol{z}(t_0) = y(t_0), \tag{A.1}$$

where $t \in [t_0, T)$, $\lambda > 0$ is an arbitrary positive number. Denote the solution of (A.1) as $\boldsymbol{z}(t, \lambda)$. It follows from Khalil (2002, Theorem 3.5) that for any $\varepsilon > 0$, there exists an $\delta > 0$ such that for $\lambda < \delta$, $|\boldsymbol{z}(t, \lambda) - \boldsymbol{y}(t)| < \varepsilon$, $\forall t \in [t_0, t_1]$ holds. Then, we have two claims stated as follows.

Claim 1: For any $\lambda > 0$, $\boldsymbol{z}(t, \lambda) - \boldsymbol{y}(t) \ge \boldsymbol{x}(t)$, $\forall t \in [t_0, t_1]$.

For any $i = 1, 2, ..., n$, if $\boldsymbol{x} \le \boldsymbol{z}$ and $x_i = z_i$ at instant t, then it follows from the condition $\frac{\partial f_i(t,\boldsymbol{x})}{\partial x_j} \ge 0$, $\forall i \ne j$, that $f_i(t, \boldsymbol{x}) \le f_i(t, \boldsymbol{z})$.

Assume Claim 1 is not true. Then, there must exist an i, an instant $t' \in [t_0, t_1)$ and a $\delta' > 0$ such that $x_i(t') = z_i(t')$, $x_i(t) > z_i(t)$ for $t \in (t', t' + \delta')$ and $x_j(t') \le z_j(t')$ for any $j \ne i$. Thus, we have $\boldsymbol{x}(t') \le \boldsymbol{z}(t')$ and $f_i(t', \boldsymbol{x}(t')) \le f_i(t', \boldsymbol{z}(t'))$. It follows from (7) that $\mathrm{D}^+ x_i(t') \le f_i(t', \boldsymbol{x}(t')) \le f_i(t', \boldsymbol{z}(t')) < f_i(t', \boldsymbol{x}(t')) + \lambda = \dot{z}_i(t')$. However, the inequality $\mathrm{D}^+ x_i(t') = \limsup_{\Delta t \to 0^+} \frac{x_i(t'+\Delta t) - x_i(t')}{\Delta t} > \limsup_{\Delta t \to 0^+} \frac{z_i(t'+\Delta t) - z_i(t')}{\Delta t} = \dot{z}_i(t')$ also holds, which yields a contradiction.

Claim 2: $\boldsymbol{y}(t) \ge \boldsymbol{x}(t)$, $\forall t \in [t_0, t_1]$.

Assume Claim 2 is not true. Then, there must exist an i and an instant $t_1' \in [t_0, t_1]$ such that $x_i(t_1') > y_i(t_1')$. Let $\varepsilon_1' = \frac{1}{2}(x_i(t_1') - y_i(t_1')) > 0$, and then there exist a $\delta' > 0$ such that $|z_i(t_1', \lambda) - y_i(t_1')| \le |\boldsymbol{z}(t_1', \lambda) - \boldsymbol{y}(t_1')| < \varepsilon_1'$ for any $\lambda < \delta'$. Thus, $z_i(t_1', \lambda) < \frac{1}{2}(x_i(t_1') + y_i(t_1')) < x_i(t_1')$, which yields a contradiction to Claim 1.

References

Anderson, B. D., Yu, C., Fidan, B., & Hendrickx, J. M. (2008). Rigid graph control architectures for autonomous formations. *IEEE Control Systems Magazine*, *28*(6), 48–63.

Ceccarelli, N., Di Marco, M., Garulli, A., & Giannitrapani, A. (2008). Collective circular motion of multi-vehicle systems. *Automatica*, *44*(12), 3025–3035.

Chen, Z., & Zhang, H.-T. (2011). No-beacon collective circular motion of jointly connected multi-agents. *Automatica*, *47*(9), 1929–1937.

Chen, Z., & Zhang, H.-T. (2013). A remark on collective circular motion of heterogeneous multi-agents. *Automatica*, *49*(5), 1236–1241.

Dorfler, F., & Francis, B. (2010). Geometric analysis of the formation problem for autonomous robots. *IEEE Transactions on Automatic Control*, *55*(10), 2379–2384.

El-Hawwary, M. I., & Maggiore, M. (2013). Distributed circular formation stabilization for dynamic unicycles. *IEEE Transactions on Automatic Control*, *58*(1), 149–162.

Hendrickx, J. M., Anderson, B., Delvenne, J.-C., & Blondel, V. D. (2007). Directed graphs for the analysis of rigidity and persistence in autonomous agent systems. *International Journal of Robust and Nonlinear Control*, *17*(10-11), 960–981.

Khalil, H. K. (2002). *Nonlinear Systems, (3rd edn)*. PrenticeHall: Upper Saddle River, NJ.

Krick, L., Broucke, M. E., & Francis, B. A. (2009). Stabilisation of infinitesimally rigid formations of multi-robot networks. *International Journal of Control*, *82*(3), 423–439.

Lan, Y., Yan, G., & Lin, Z. (2010). Distributed control of cooperative target enclosing based on reachability and invariance analysis. *Systems & Control Letters*, *59*(7), 381–389.

Lee, B.-H., & Ahn, H.-S. (2016). Distributed formation control via global orientation estimation. *Automatica*, *73*, 125–129.

Lin, Z., Broucke, M., & Francis, B. (2004). Local control strategies for groups of mobile autonomous agents. *IEEE Transactions on Automatic Control*, *49*(4), 622–629.

Marshall, J. A., Broucke, M. E., & Francis, B. A. (2004). Formations of vehicles in cyclic pursuit. *IEEE Transactions on Automatic Control*, *49*(11), 1963–1974.

Marshall, J. A., Broucke, M. E., & Francis, B. A. (2006). Pursuit formations of unicycles. *Automatica*, *42*(1), 3–12.

Narendra, K. S., & Annaswamy, A. M. (1987). Persistent excitation in adaptive systems. *International Journal of Control*, *45*(1), 127–160.

Oh, K.-K., & Ahn, H.-S. (2013). Formation control of mobile agents based on distributed position estimation. *IEEE Transactions on Automatic Control*, *58*(3), 737–742.

Oh, K.-K., Park, M.-C., & Ahn, H.-S. (2015). A survey of multi-agent formation control. *Automatica*, *53*, 424–440.

Qu, Z. (2009). *Cooperative control of dynamical systems: applications to autonomous vehicles*. Springer.

Sepulchre, R., Paley, D. A., & Leonard, N. E. (2007). Stabilization of planar collective motion: All-to-all communication. *IEEE Transactions on Automatic Control*, *52*(5), 811–824.

Sepulchre, R., Paley, D. A., & Leonard, N. E. (2008). Stabilization of planar collective motion with limited communication. *IEEE Transactions on Automatic Control*, *53*(3), 706–719.

Seyboth, G. S., Wu, J., Qin, J., Yu, C., & Allgower, F. (2014). Collective circular motion of unicycle type vehicles with non-identical constant velocities. *IEEE Transactions on Control of Network Systems*, *1*(2), 167–176.

Sinha, A., & Ghose, D. (2007). Generalization of nonlinear cyclic pursuit. *Automatica*, *43*(11), 1954–1960.

Su, Y., & Huang, J. (2012). Cooperative output regulation of linear multi-agent systems. *IEEE Transactions on Automatic Control*, *57*(4), 1062–1066.

Summers, T. H., Akella, M. R., & Mears, M. J. (2009). Coordinated standoff tracking of moving targets: control laws and information architectures. *Journal of Guidance, Control, and Dynamics*, *32*(1), 56–69.

Wang, K., Liu, Y., & Li, L. (2014). Visual servoing trajectory tracking of nonholonomic mobile robots without direct position measurement. *IEEE Transactions on Robotics*, *30*(4), 1026–1035.

Yu, X., & Liu, L. (2016a). Distributed circular formation control of ring-networked nonholonomic vehicles. *Automatica*, *68*, 92–99.

Yu, X., & Liu, L. (2016b). Distributed formation control of nonholonomic vehicles subject to velocity constraints. *IEEE Transactions on Industrial Electronics*, *63*(10), 1289–1298.

Zhang, H., Li, Z., Qu, Z., & Lewis, F. L. (2015). On constructing Lyapunov functions for multi-agent systems. *Automatica*, *58*, 39–42.

Zheng, R., Lin, Z., & Yan, G. (2009). Ring-coupled unicycles: boundedness, convergence, and control. *Automatica*, *45*(11), 2699–2706.

Zheng, R., Liu, Y., & Sun, D. (2015). Enclosing a target by nonholonomic mobile robots with bearing-only measurements. *Automatica*, *53*, 400–407.